Polysulfone-iron acetate/polyamide nanocomposite membrane for oil-water separation

Hamouda M. Mousa[a,b,*], Husain Alfadhel[b], Mohamed Ateia[c], G.T. Abdel-Jaber[a], Gomaa A. A[d]

[a] Department of Engineering Materials and Mechanical Design, Faculty of Engineering, South Valley University, Qena 83523, Egypt
[b] Department of Mechanical Engineering, Massachusetts Institute of Technology, Cambridge, MA, United States
[c] Department of Chemistry, Northwestern University, Evanston, IL 60208, United States
[d] Department of Mechanical Engineering "Mechatronics Branch", El-Minia High Institute for Engineering & Technology, 61111 El-Minia, Egypt

ARTICLE INFO

ABSTRACT

Polysulfone (PSF) membranes are widely used for water filtration, however, their hydrophobic nature limits their application in oil-water separation. Herein, we report on the preparation of hydrophilic, high-flux and mechanically-stable PSF-based nanofiber membrane. The membrane was fabricated via electrospinning of a PSF solution containing iron acetate powder followed by deposition of a polyamide (PA) layer using interfacial polymerization on both sides of the membrane. This treatment resulted in switching membrane from being hydrophobic (contact angle = 100 ± 7°) to be highly hydrophilic (contact angle = 37 ± 5°) and the membrane porosity reached up to 83 ± 7 % after the deposition of the PA layer. Results from field emission electron microscopy with energy dispersive spectroscopy (FESEM-EDS), transmission electron microscopy (TEM), and X-ray photoelectron spectroscopy (XPS) showed the unique nanofiber characteristics with uniform iron distributions. The new membranes have also improved mechanical properties as indicated by Young's modulus and mechanical strength. In addition, the membranes efficiently separated water from oil-water mixtures and the water flux of the modified membrane was three times higher than the unmodified PSF membrane in this study and also higher than previously reported membranes.

1. Introduction

Oil-water separation is considered as a major environmental challenge due to the notable increase in industrial oily wastewater release as well as the frequent crude oil leakage (Obaid et al., 2015b). Depending on the oil's drop-size, three main classifications are being used to describe water contamination with oil: 1) Free Oil with drop-size > 150 μm, 2) dispersed oil with drop size-range from 20 μm to 150 μm, and 3) emulsified oil with drop-size < 20 μm (Cheryan and Rajagopalan, 1998). It should be highlighted that the recommended oil in water mixture concentrations should not exceed 15 mg/l, regardless of the oil drop size (Su et al., 2012). To this end, membrane technology is considered as a green and effective separation method that can be used in treatment of oily wastewater without any chemical addition or sludge production (Zhao et al., 2014). There are several commercial materials for membranes; such as cellulose acetate, polyvinylidene fluoride, polyetherimide, aromatic polyamides, and polysulfone (PSF) (Obaid et al., 2015c). Among them, PSF is an amorphous polymer that is widely used as a membrane material in ultrafiltration membranes,

nanofiltration, and as a support layer in reverse osmosis (RO) filtration due to its excellent mechanical properties and chemical stability (Obaid et al., 2015b). However, low flux, degradation, concentration polarization, and hydrophobicity of PSF membranes are the main challenges that face their design, fabrication, and application for oil-water separation (Ulbricht, 2006; Zhao et al., 2011). Thus, these limitations need innovative techniques and materials with improved surface hydrophilicity via interfacial polymerization and/or the incorporation of hydrophilic nanoparticles (Panda and De, 2014; Song et al., 2014; Wang et al., 2014).

Membrane fabrication by means of hydrodynamic electrospinning characterized with high surface area, which attracted much attention for their practical applications as high-performance filter media for water treatment. During electrospinning process, the generated electrostatic force overcome the surface tension of the viscous solution, this followed by ejection of thin jet of nanofiber which collected on the grounded target (Rezk et al., 2019). Deposition of polyamide (PA) layer on the polysulfone membrane work as a hydrophilic layer as well as it exhibits a moderate to strong anionic surface charge (Scott, 1995).

* Corresponding author at: Department of Engineering Materials and Mechanical Design, Faculty of Engineering, South Valley University, Qena 83523, Egypt.
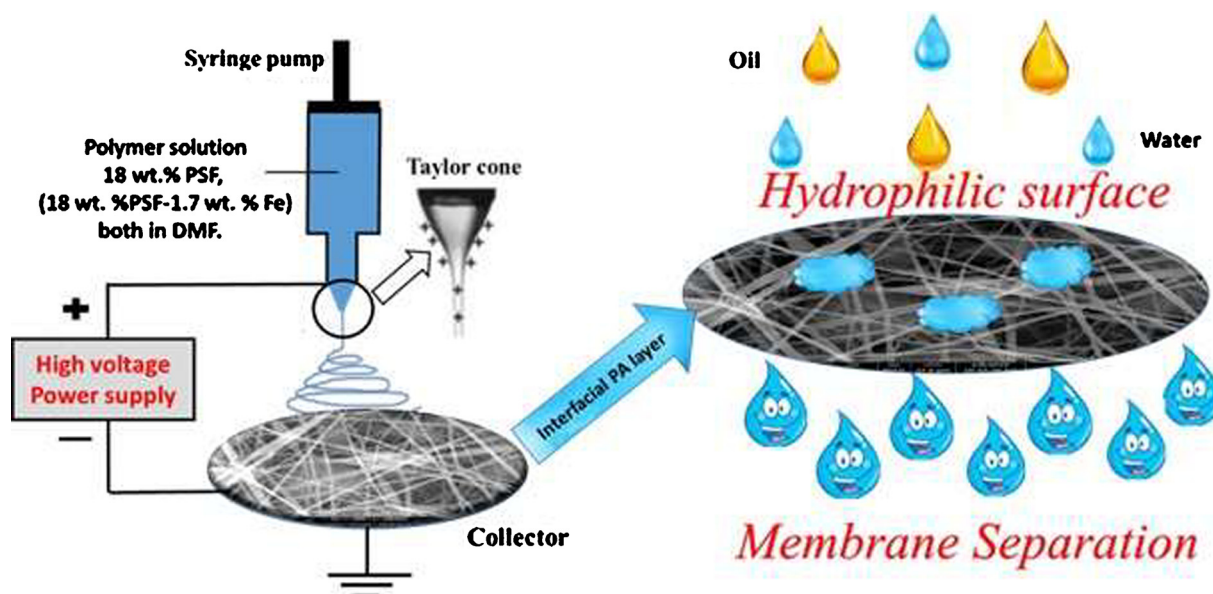E-mail addresses: hamouda@mit.edu, hmousa@eng.svu.edu.eg (H.M. Mousa).

Fig. 1. Illustration of the electrospinning setup for membrane fabrication followed by PA film formation and oil/water separation.
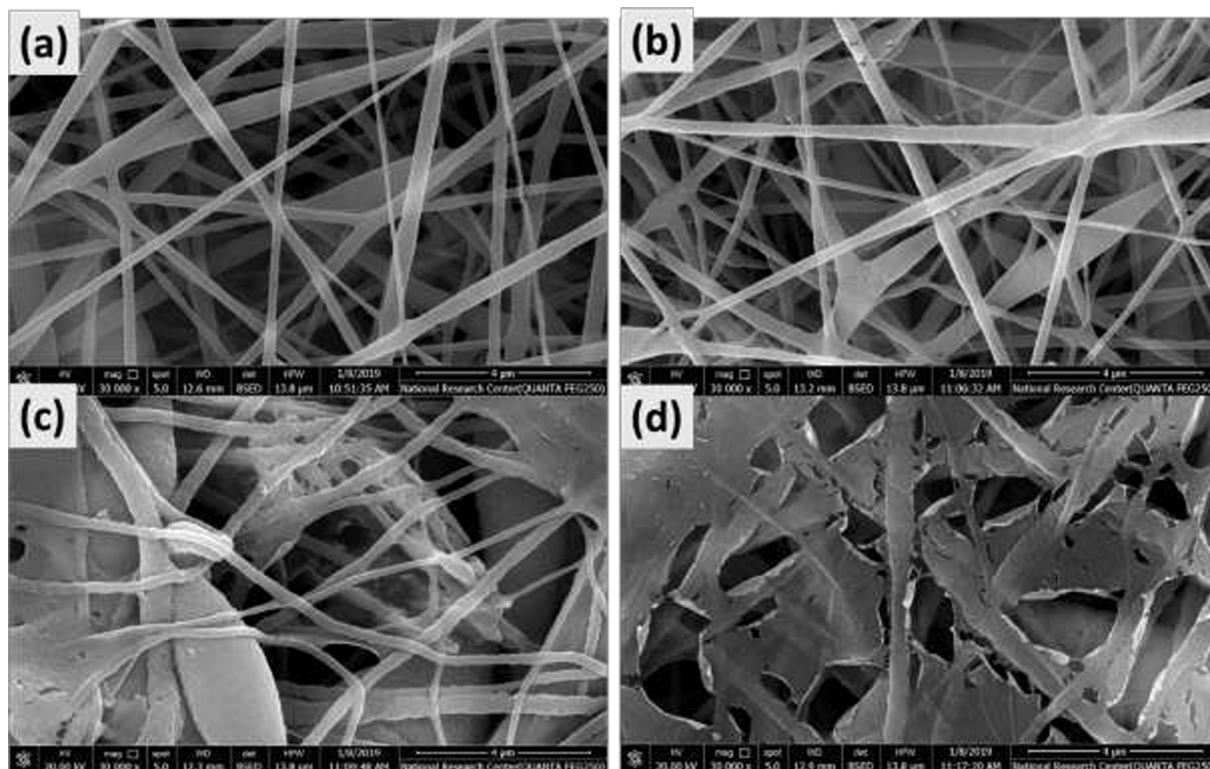

Fig. 2. FESEM images of different membrane (a) PSF, (b) PSF-Fe, and (c,d) Coated membrane in (a, b) with PA layer.

Composite membranes are widely fabricated by adding inorganic nanoparticles; however, this method faces several challenges about particles aggregation, nanoparticles cost, and decrease in membrane mechanical properties (Akther et al., 2019; Safarpour et al., 2014). A previous study by (Eid et al., 2010) showed that 1D nanostructure materials can be prepared after different annealing processes of polyvinyl pyrrolidone and iron acetate nanofibers. 1D nanostructures contained α-Fe_2O_3 nanotubes with a tunable wall thickness and polycrystalline Fe_3C nanofibers. Inspired by these observations, we report herein on the fabrication of a novel PSF-based membranes via electrospinning of PSF solution with/without iron acetate followed by

interfacial polymerization of polyamide layer on the membrane surface. We hypothesized that resulted membranes would have promising advantages comparing to those prepared by substitution of nanoparticles that can aggregate and are more expensive than iron acetate salt. Furthermore, membrane could enhance various properties such as; mechanical properties, hydrophilicity, oil-water separation, and water flux.
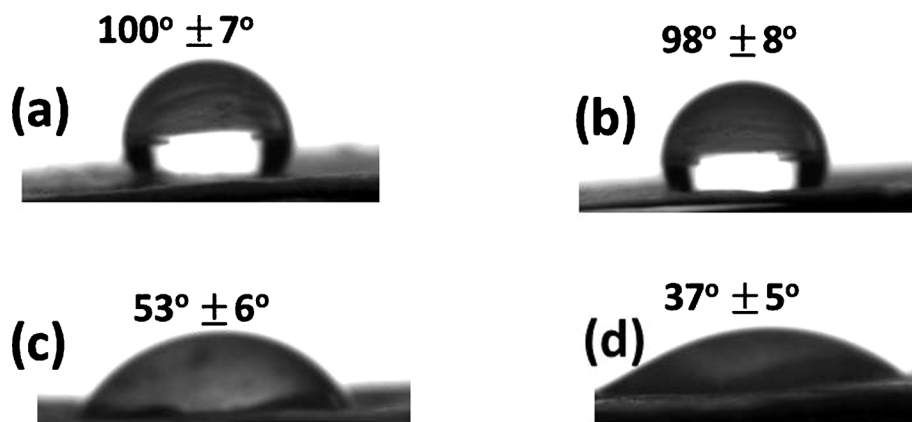
Fig. 3. WCA measurements for the different membranes: (a) PSF, (b) PSF-Fe, and (c,d) Coated PA layer membrane.

Table 1
Membrane Characteristics.

Membrane materials	Membrane Characteristics		
	Thickness (μm)	Porosity (%)	Average Fiber diameter (nm)
PSF	80 ± 4	75 ± 6	261 ± 50
PSF/Iron acetate	85 ± 8	79 ± 5	219 ± 20
PSF/ PA film	82 ± 6	80 ± 4	–
PSF/Iron acetate/ PA film	88 ± 5	83 ± 7	–

2. Materials and methods

2.1. Materials

PSF and N, N-dimethylformamide (DMF) were purchased from Sigma Aldrich and used to prepare the electrospun membrane. Iron (II) acetate (Fe (CH_3O_2), Sigma Aldrich.), P-Phenylenediamine (PPD), and 1,3,5-Benzenetricarbonyl chloride (TMC) from Sigma Aldrich were utilized in the electrospun membrane coating.

2.2. Membrane fabrication

The membranes were prepared by dissolving 18 wt.% of PSF in DMF to obtain PSF viscous solution then mixed with 1.7 wt. % of iron acetate salt dissolved in DMF. Solution color was changed to red–brown after addition of iron acetates. The prepared solution was loaded into a plastic syringe pump and electrospun at 18 Kv with 15 cm distance away from the collector by using a pumping flow rate of 0.1 mL/h (Supplier: NanoNC, South Korea). The fabricated nanofibers were collected and then dried in a vacuum oven at 70 °C. The dried electrospun membrane was deposition by a thin polyamide (PA) layer as follows: First, 0.2 % (w/v) MPD aqueous solution was soaked onto the top surface of the membrane and the solution was stacked on the surface for
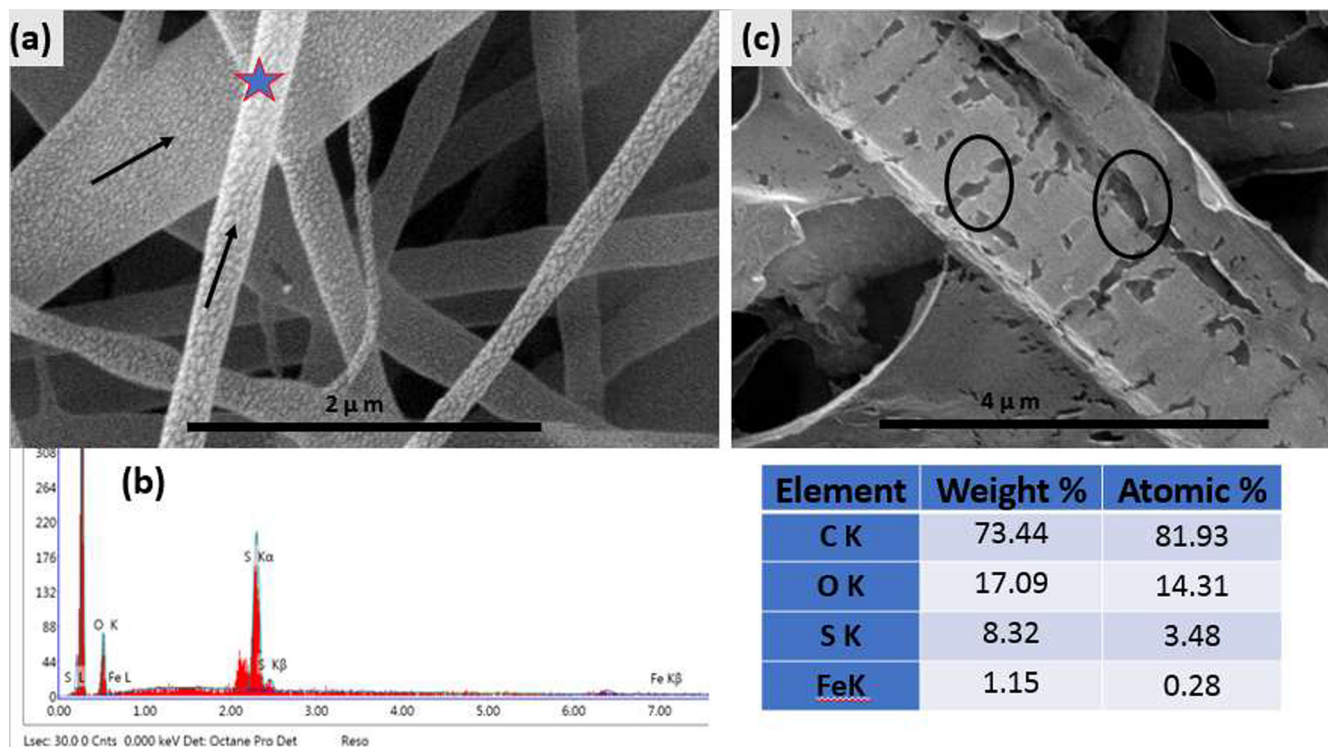

Element	Weight %	Atomic %
C K	73.44	81.93
O K	17.09	14.31
S K	8.32	3.48
FeK	1.15	0.28

Fig. 4. (a, b) high magnification of PSF-Fe membrane before and after activation, EDS point (Star on the fiber) of the PSF-Fe membrane, arrows refer to iron nanocrystals on the outer fibers.
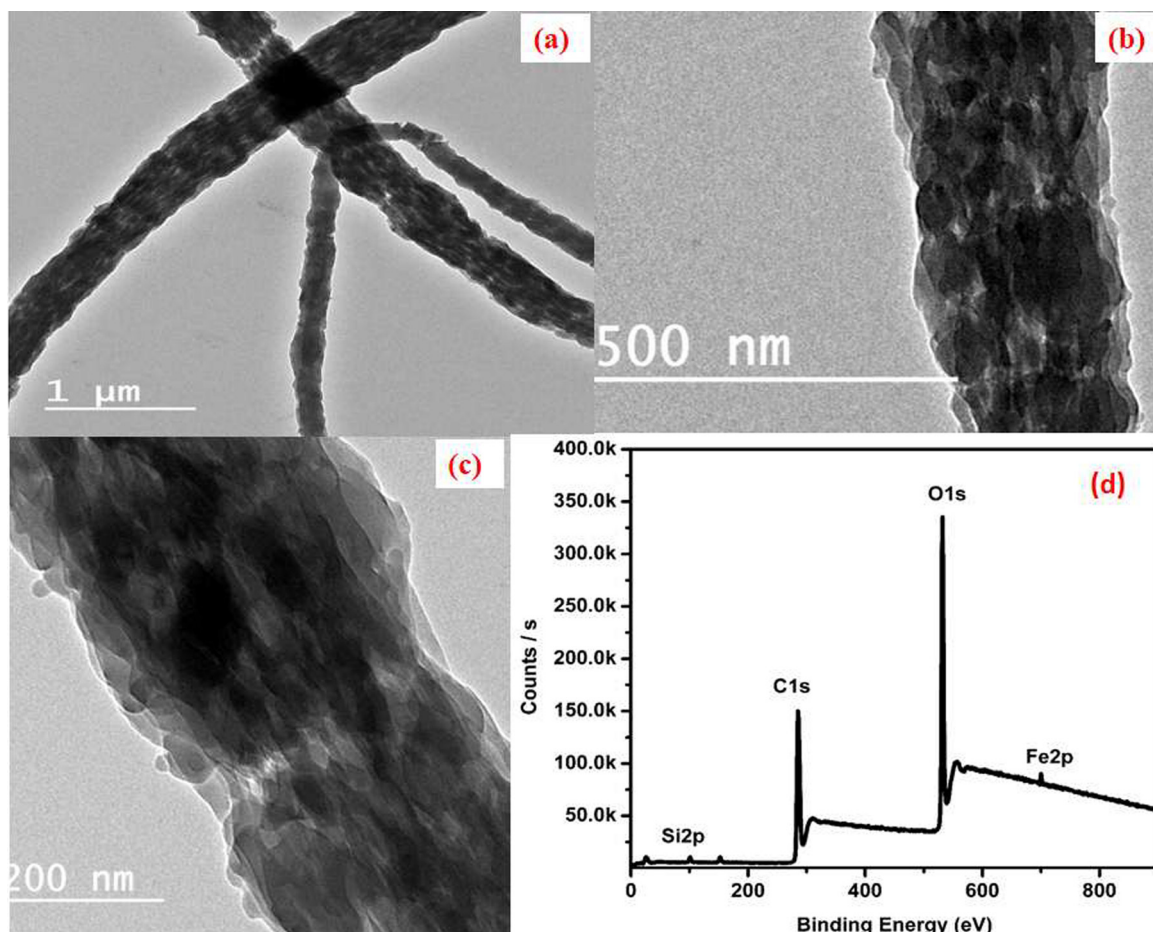
Fig. 5. Characterization of PSF-Fe acetate nanofiber: (a–c) Different TEM images resolution, (d) XPS wide scan results.

2 min, after that TMC solution (0.02 % (w/v) in hexane) was poured onto the substrate surface. After 1 min, the TMC solution was then drained off from the surface of the membranes. Hereafter, the membranes will be called as PSF, PSF-Fe, coated PSF and coated PSF-Fe for the main membranes and their coated surfaces. Finally, the membrane was washed in distilled water and stored until further use. A graphical description of the preparation method is shown in Fig. 1.

2.3. Membrane characterizations

The membranes surface morphology was observed by FE-SEM and EDS point (QUANTA FEG 250, Thermo Scientific™ Quanta™, USA). A DPRO image standard goniometer device (Rame' Hart, Mountain Lakes, NJ, and USA) was used to measure the water contact angle. Fourier-transform infrared spectroscopy (FTIR) (Shimadzu FTIR-8400 S, Japan), Surface chemistry of membrane was studied by using X-ray photoelectron spectroscopy (XPS, AXISNOVA, Kratos, Inc.) with an Al Kα irradiation source. X-ray diffraction (Empyrean, Malvern Panalytical Ltd, UK) were used for membrane crystallinity. The mechanical properties of the fabricated membranes were performed using a tensile tester (model AG-I, Shidmadzu, Japan) according to ASTM ID: D882−12. The oil-water separation process was achieved in a permeation cell having a total effective round area with 19.6 cm^2. Membrane thickness was assessed by coating thickness gauge meter (Elcometer 456, Accuracy: ± (3% +2 μm)). Membrane porosity calculated according to the previous report (Abdal-hay et al., 2015).

Density of membrane (g/cm3) $= \frac{membrane\ mass\ (g)}{membrane\ thicknes\ (cm) \times membrane\ area\ (cm2)}$

Porosity (%) $= 1 - \frac{denesity\ of\ membrane\ (g/cm^3)}{denesity\ of\ used\ membrane\ (g/cm^3)}$

2.4. Membrane performance evaluation

A laboratory scale permeation cell was setup to evaluate membrane capability to separate oil from water and oil water separation process. Membranes were tested for oil-water separation in the water-oil mixture (3:1 vol ratio) and the water flux was calculated using Eq. (1).

$$J = \frac{Q}{A \times t}$$ (1)

Where: J is water flux (m^3. m^{-2}. h^{-1}), Q is water quantity in m^3, A is the surface area, t is the time (h). The oil-water separation process was achieved in a permeation cell having a total effective round area with 19.6 cm^2. The oil type used in this study was a commercial sunflower oil and all chemicals and reagents used in this study were of analytical grade and used as received without further purification.

3. Results and discussions

3.1. Membrane physiochemical characterization

PSF membranes had bead-free nanofibers and the addition of iron acetate resulted in the formation of nanocrystals on the nanofibers outer surface. This nanocrystal attributed to dissolve of iron acetate on the polymer solution and form tinny crystals of iron ions. Fig. 2a and b show the FE-SEM images of the PSF, PSF-Iron acetate, and the interfacial polymerized PA thin film of the two nanofibers membranes. The chemically coated membranes with the PA film are shown in Fig. 2(c and d) with discontinues fibers and film formations on the top layer. Membrane water permeation determined by membrane hydrophilicity. In most cases, membrane with hydrophobic properties decrease water
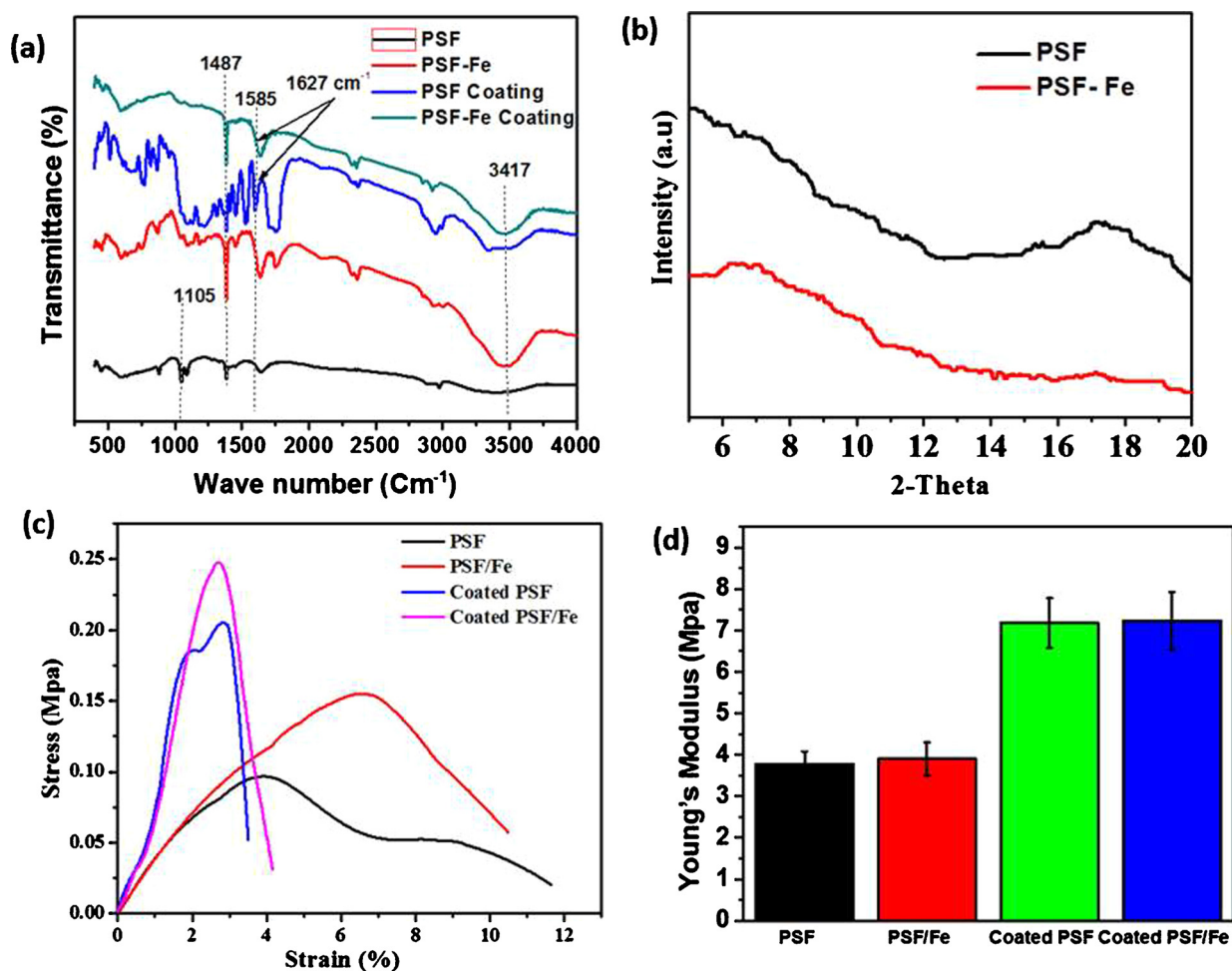
Fig. 6. (a) FTIR spectra analysis, (b) XRD analysis, (c) stress & strain curve, and (d) membranes Young's modulus.

permeation and increase fouling, however hydrophilic membranes have higher surface energy and lower water contact angle (WCA) (Liu et al., 2012). The pristine PSF membrane showed the highest WCA of about $100 \pm 7°$, and addition of iron acetate show slightly decrease in WCA to about 98 ± 8. The PA layer on the composite membrane (PSF/Iron acetate) drastically change the membrane to hydrophilic $37 \pm 5°$ as shown in Fig. 3. This is consistent with the previous reports which showed that incorporation of inorganic particles and within the membrane fibers and PA polymeric layer enhances the membrane hydrophilicity (Cui et al., 2008; Yang et al., 2018).

Membrane characterizations in terms of thickness, porosity, and fiber diameter are appended in Table 1. The chemically coated composite membrane with PA layer was found to have about $88 \pm 5 \mu m$ of thickness and $83 \pm 7\%$ of porosity higher than pristine PSF membrane (thickness = $80 \pm 4 \mu m$, porosity of $75 \pm 6\%$). These results revealed increasing of membrane porosity and thus increasing membrane water permeation. Membranes nanofibers were measured using FE-SEM software interface (Fig. S1 and S2, supporting information) with and without the addition of iron acetate. The average diameters of membrane nanofibers were $261 \pm 50 nm$ attributed to PSF and $219 \pm 20 nm$ for PSF-iron acetate membranes. Fig. 4a indicates the outer fibers surface of membrane contains tinny iron particles (indicated by the referred arrows in the enlarged FE-SEM images). Fig. 4b shows EDS analysis of the PSF/ iron acetate membrane, the main elemental weight percent was C, O, Si, Fe with 73.44 %, 17.09 %, 8.32 %, and 1.15 %, respectively. Chemical formation of PA layer on the composite PSF/iron acetate affect the fiber morphology by forming nano-porous structure on the fiber surface as shown in referred circles

in Fig. 4c.

Fig. 5(a–c) show different TEM images magnification of PSF-Fe acetate that illustrate a homogenous composite nanofiber. This indicate that iron acetate can homogenously distributed along with the electrospinning composite polymeric solution (before subject to electrostatic force of electrospinning); and resulted in a polymeric nanofibers based iron salt without any agglomeration which usually occurs with nanoparticles (Mahmoudi et al., 2019). XPS scan in Fig. 5d mainly show a high intensity peaks of C1s, O1S, and two low intensity peaks of Si2p and Fe2p$_{3/2}$. The determined binding energies of Si2p and Fe2p$_{3/2}$ are 103.1 (assigned to O–Si–O in PSF polymer) and 711.1 eV, respectively (Fu et al., 2017). Additionally, the elemental fine spectra of C1s, O1s, Fe2p are appended in Figs. S4-S6 (Supporting information). Membrane characterization is appended in Table S1, the atomic weight percent are 63.28, 36.28, and 0.44 for C1s, O1s, and Fe2p, respectively. Both TEM and XPS results revealed formation of iron particles among the composite nanofibers.

Membranes characteristics changes on the fibers diameters values are mainly attributed to the presence of iron acetate on the polymeric solution. The mechanism of electrospinning based on applying high potential on the syringe solution and collector with negative charge as grounded collector. Thus presence of Fe + ions increase polymeric solution conductivity which is essential factor in electrospinning. Additionally, the positive ions of iron salt after totally dissolve form tinny crystals among fibers and outer surface. This concludes that iron acetate has a direct influence on both spinning process (i.e. fiber size and morphology) and surface tension of the membrane surface (i.e. surface wettability) and exhibit slightly low contact angle. This might

Table 2
Comparison between the present membrane properties and some recent reported membranes.

Materials	Water Flux (m³·m⁻²·hr⁻¹)	Technique	Tensile stress (MPa)	WCA	Separated Compound	Membrane features	Ref.
PVDF-TiO₂ composite membrane	0.072	Dry-jet wet spinning	2.05 ± 0.16	59.95° ± 1.34°	emulsion synthesized from cutting oil	Moderate hydrophilic, Particles may agglomeration	(Ong et al., 2014)
PSF /NaOH	0.33	Electrospinning	1.10	12°	Soybean oil	High flux, Super hydrophilic	(Obaid et al., 2015a)
(PSF/NaOH) PA layer	0.33		–	3 °	Soybeanoil	Super hydrophilic	(Obaid et al., 2015c)
PSF	0.14		0.9	100°	Sunflower oil	Hydrophobic, degradation by oil, heat resistance, pH resistance	This study
PSF/Iron acetate	0.17		0.16	98°		Hydrophobic	This study
PSF/ PA film	0.31		0.2	53°		Moderate hydrophilic	This study
PSF/Iron acetate/ PA film	0.38		0.25	37°		High flux, low cost of salt comparing to nanoparticles, hydrophilic, avoid particles agglomeration	This study

be due to the presence of iron salt in the polymeric solution in the Taylor cone (end of the syringe) as shown in Fig. 1 and in the resulted FE-SEM image (Fig. S3, supporting information) has much higher acceleration on fiber formation (Barakat et al., 2009). It is noteworthy mentioning that this is the first attempt to use iron acetate, which is cheap comparing to nanoparticles and easy to process in organic solvent for the preparation of a composite PSF nanofiber membrane. This gives an extra advantage to the present membrane material comparing to the previously reported composites that used nanoparticles of iron oxide (Said et al., 2017) or silica (Obaid et al., 2015d) to achieve the same enhancement in PSF in terms of materials cost and membrane characteristics.

FTIR spectra of the different PSF membranes is shown in Fig.6(b), peaks at $3417 \, cm^{-1}$ refer to C−OH vibration and peaks at $1585 \, cm^{-1}$ and $1487 \, cm^{-1}$ located in the four membranes corresponding to stretching of aromatic ring quadrant and stretching of aromatic semi-ring, respectively (Huang et al., 2013). In addition, peaks at $1105 \, cm^{-1}$ attributed to S=O symmetric stretching in polysulfone structure (Kang et al., 2018). The coated membranes showed a peak at $1627 \, cm^{-1}$ attributed to C=O stretching vibration of amide, which confirms and evidence of the formation of PA film on the membranes (Ruan et al., 2018). X-ray diffraction in Fig. 6(c) shows that the PSF generally has an amorphous structure and there were no major changes after addition of iron acetate to the polymer solution due to the low concentration of iron in polymer solution before electrospining setup.

3.2. Mechanical properties of the membranes

Membrane mechanical properties is an important aspect in membrane applications, durability, and process-ablity. Fig. 6(c) show mechnical properties of the fabircated membranes in terms of stress and strian. The addition of iron acetate decreased the strain and increased the tensile stress three times comparing to the pristine PSF membrane. Moreover, there are no changes in the elastic behavior of the PSF composite as indicated by the similar values of Young's modulus Fig. 6(d), which attributed to the nanofiber diameters and membrane porosity (Obaid et al., 2015a). On the other hand, the PA layer show a typical higher tensile stress and Young's modulus in both cases. Ths is due to interfacial interaction between the polymer matrix and its composite with a new PA film with hydroxide groups (Huang et al., 2017). Conversely, the membrane strain was decreased, this suggested that formation of brittle behavior and increasing of mechanical strength.

3.3. Membrane oil-water separation

There are many factors and parameters that affect the membrane design should be considered (i.e., membrane material, separation method, surface properties, target contaminant, water pH, and mechanical properties) (Ge et al., 2019). Previous studies listed in Table 2 show that there are many oil type that can be used to stimulate oil/water separation that include emulsion synthesized from cutting oil, n-hexane, soybean oil, and sunflower oil. Besides, the comparison studies ware performed under two techniques which are dry-jet wet spinning and electrospinning.

Inorganic nanomaterials are widely used in membrane technology to improve specific properties such as hydrophilicity, antibacterial properties, mechanical strength, antifouling, and membrane structure (Akther et al., 2019). Herein, the coated PSF-Fe membrane had the highest water flux $(0.38 \, m^3 \cdot m^{-2} \cdot h^{-1})$ among the four tested membranes in this study, which was attributed to the enhanced membrane hydrophilicity Fig. 7. In addition, a comparison between our membrane and previous studies is summarized in Table 2. For instance, membrane composed from (PSF/NaOH) /coated with PA layer, a composite PVDF-TiO₂ membrane, PSF/NaOH has 0.33, 0.072, and $0.33 \, m^3 \cdot m^{-2} \cdot h^{-1}$ of water flux, respectively. Thus, our developed membrane exhibited higher water flux values in oil-water separation than the previously
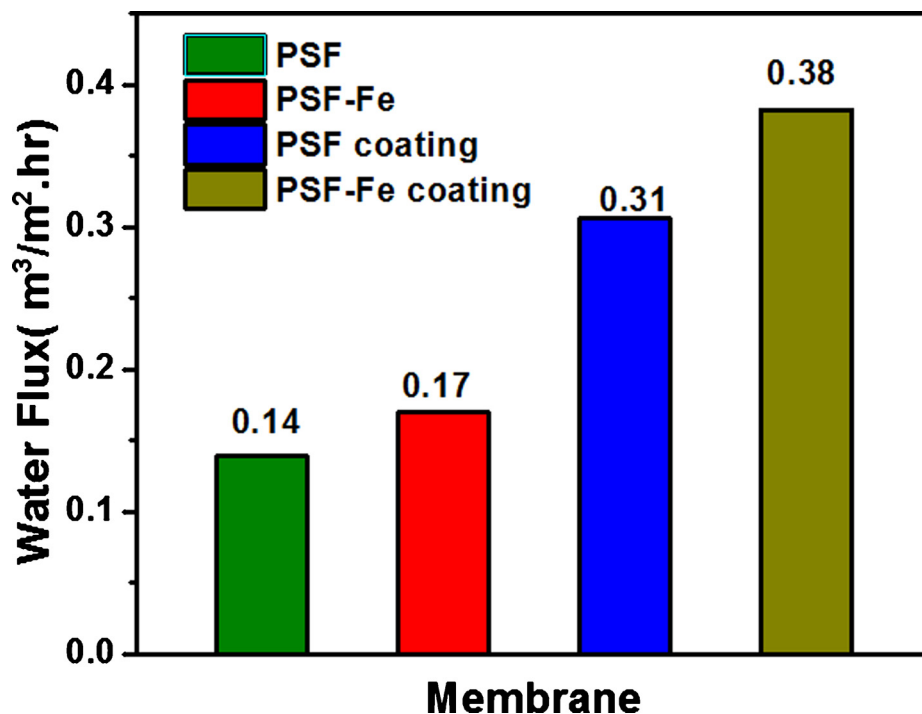
Fig. 7. Membrane water flux in the water-oil mixture separation process.
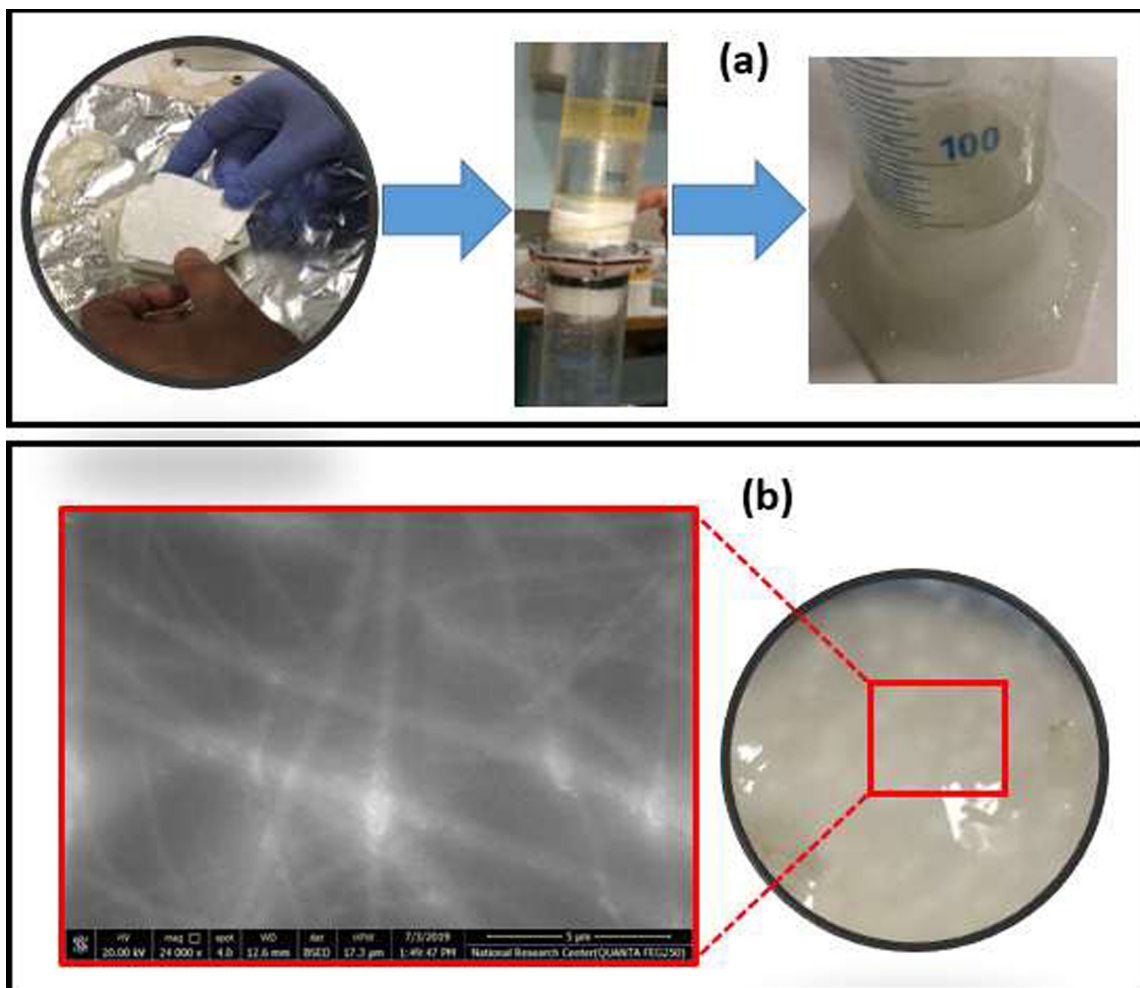

Fig. 8. (a) Optical of permeation oil/water separation, and (b) FESEM images of (PSF/Fe) membrane in oil/water after one cycle of separation.

reported membranes. This attributed to membrane composite structure that can provide sufficient physiochemical properties. Membrane with functional (amide and OH-) groups of the polyamide layer enhance surface hydrophilicity and resulted in sufficient porosity percentage as shown in Table 1 which subsequently increased the water flux (Laurati et al., 2012). Furthermore, membrane maintained a morphology close its initial state after one cycle which is clear in Fig. 8(a and b) and covered with minor oil in the outer surface which account to its degradation stability.

4. Conclusions

In this study, PSF electrospun membrane with iron acetate composite could significantly enhance the fiber distribution and the membrane performance in both mechanical properties and water flux. The findings from this studies were summarized as follows:

- Coating the membrane with a PA interfacial polymerization played a vital role in the surface hydrophilicity (contact angle decreased from $100 \pm 7°$ to $37 \pm 5°$) and subsequently increase in water flux (0.38 $m^3 . m^{-2} . h^{-1}$).
- All the physical and chemical treatments in the present study resulted in improved young modules and membrane stability.
- Overall, the proposed membrane fabrication strategy is facile and can introduce PSF membranes and their alternative composites to be used in different industrial applications. Moreover, the novel nanofiber membrane developed in this work is a potential alternative tool for membrane application in water application especially oil/water separation.

CRediT authorship contribution statement

Hamouda M. Mousa: Conceptualization, Methodology, Software, Data curation, Writing - original draft, Resources. **Husain Alfadhel:** Methodology, Writing - review & editing, Resources. **Mohamed Ateia:** Writing - review & editing. **G.T. Abdel-Jaber:** Writing - review & editing. **Gomaa A. A:** Writing - review & editing.

Declaration of Competing Interest

The authors declare that they have no known competing financial interests or personal relationships that could have appeared to influence the work reported in this paper.

Appendix A. Supplementary data

Supplementary material related to this article can be found, in the online version, at doi:https://doi.org/10.1016/j.enmm.2020.100314.

References

Abdal-hay, A., Hamdy Makhlouf, A.S., Khalil, K.A., 2015. Novel, facile, single-step technique of Polymer/TiO2 nanofiber composites membrane for photodegradation of methylene blue. ACS Appl. Mater. Interfaces 7 (24), 13329–13341. https://doi.org/10.1021/acsami.5b01418.

Akther, N., Phuntsho, S., Chen, Y., Ghaffour, N., Shon, H.K., 2019. Recent advances in nanomaterial-modified polyamide thin-film composite membranes for forward osmosis processes. J. Memb. Sci. 584, 20–45. https://doi.org/10.1016/j.memsci.2019.04.064.

Barakat, N.A.M., Kanjwal, M.A., Sheikh, F.A., Kim, H.Y., 2009. Spider-net within the N6, PVA and PU electrospun nanofiber mats using salt addition: novel strategy in the electrospinning process. Polymer 50 (18), 4389–4396. https://doi.org/10.1016/j.polymer.2009.07.005.

Cheryan, M., Rajagopalan, N., 1998. Membrane processing of oily streams. Wastewater treatment and waste reduction. J. Memb. Sci. 151 (1), 13–28. https://doi.org/10.1016/S0376-7388(98)00190-2.

Cui, W., Li, X., Zhou, S., Weng, J., 2008. Degradation patterns and surface wettability of electrospun fibrous mats. Polym. Degrad. Stab. 93 (3), 731–738. https://doi.org/10.1016/j.polymdegradstab.2007.12.002.

Eid, C., Brioude, A., Salles, V., Plenet, J.-C., Asmar, R., Monteil, Y., et al., 2010. Iron-based

1D nanostructures by electrospinning process. Nanotechnology 21 (12), 125701. https://doi.org/10.1088/0957-4484/21/12/125701.

Fu, H., Ding, X., Ren, C., Li, W., Wu, H., Yang, H., 2017. Preparation of magnetic porous NiFe2O4/SiO2 composite xerogels for potential application in adsorption of Ce(iv) ions from aqueous solution. RSC Adv. 7 (27), 16513–16523. https://doi.org/10.1039/C6RA27219C.

Ge, J., Fu, Q., Yu, J., Ding, B., 2019. Chapter 13 - electrospun nanofibers for Oil–Water separation. In: Ding, B., Wang, X., Yu, J. (Eds.), Electrospinning: Nanofabrication and Applications. William Andrew Publishing, pp. 391–417.

Huang, T., Zhang, M., Cheng, L., Zhang, L., Huang, M., Xu, Q., Chen, H., 2013. A novel polysulfone-based affinity membrane with high hemocompatibility: preparation and endotoxin elimination performance. RSC Adv. 3 (48), 25982–25988. https://doi.org/10.1039/C3RA43594F.

Huang, N.-J., Zang, J., Zhang, G.-D., Guan, L.-Z., Li, S.-N., Zhao, L., Tang, L.-C., 2017. Efficient interfacial interaction for improving mechanical properties of poly-dimethylsiloxane nanocomposites filled with low content of graphene oxide nanoribbons. RSC Adv. 7 (36), 22045–22053. https://doi.org/10.1039/C7RA02439H.

Kang, Y., Obaid, M., Jang, J., Ham, M.-H., Kim, I.S., 2018. Novel sulfonated graphene oxide incorporated polysulfone nanocomposite membranes for enhanced-performance in ultrafiltration process. Chemosphere 207, 581–589. https://doi.org/10.1016/j.chemosphere.2018.05.141.

Laurati, M., Sotta, P., Long, D.R., Fillot, L.A., Arbe, A., Alegrìa, A., et al., 2012. Dynamics of Water Absorbed in Polyamides. Macromolecules 45 (3), 1676–1687. https://doi.org/10.1021/ma202368x.

Liu, Y., Yue, X., Zhang, S., Ren, J., Yang, L., Wang, Q., Wang, G., 2012. Synthesis of sulfonated polyphenylsulfone as candidates for antifouling ultrafiltration membrane. Sep. Purif. Technol. 98, 298–307. https://doi.org/10.1016/j.seppur.2012.06.031.

Mahmoudi, E., Ng, L.Y., Ang, W.L., Chung, Y.T., Rohani, R., Mohammad, A.W., 2019. Enhancing morphology and separation performance of polyamide 6,6 membranes by minimal incorporation of silver decorated graphene oxide nanoparticles. Sci. Rep. 9 (1), 1216. https://doi.org/10.1038/s41598-018-38060-x.

Obaid, M., Barakat, N.A.M., Fadali, O.A., Al-Meer, S., Elsaid, K., Khalil, K.A., 2015a. Stable and effective super-hydrophilic polysulfone nanofiber mats for oil/water separation. Polymer 72, 125–133. https://doi.org/10.1016/j.polymer.2015.07.006.

Obaid, M., Barakat, N.A.M., Fadali, O.A., Motlak, M., Almajid, A.A., Khalil, K.A., 2015b. Effective and reusable oil/water separation membranes based on modified polysulfone electrospun nanofiber mats. Chem. Eng. J. 259, 449–456. https://doi.org/10.1016/j.cej.2014.07.095.

Obaid, M., Fadali, O.A., Lim, B.-H., Fouad, H., Barakat, N.A.M., 2015c. Super-hydrophilic and highly stable in oils polyamide-polysulfone composite membrane by electrospinning. Mater. Lett. 138, 196–199. https://doi.org/10.1016/j.matlet.2014.09.121.

Obaid, M., Tolba, G.M.K., Motlak, M., Fadali, O.A., Khalil, K.A., Almajid, A.A., et al., 2015d. Effective polysulfone-amorphous SiO2 NPs electrospun nanofiber membrane for high flux oil/water separation. Chem. Eng. J. 279, 631–638. https://doi.org/10.1016/j.cej.2015.05.028.

Ong, C.S., Lau, W.J., Goh, P.S., Ng, B.C., Matsuura, T., Ismail, A.F., 2014. Effect of PVP molecular weights on the properties of PVDF-TiO2 composite membrane for oily wastewater treatment process. Sep. Sci. Technol. 49 (15), 2303–2314. https://doi.org/10.1080/01496395.2014.928323.

Panda, S.R., De, S., 2014. Preparation, characterization and performance of ZnCl2 incorporated polysulfone (PSF)/polyethylene glycol (PEG) blend low pressure nanofiltration membranes. Desalination 347, 52–65. https://doi.org/10.1016/j.desal.2014.05.030.

Rezk, A.I., Mousa, H.M., Lee, J., Park, C.H., Kim, C.S., 2019. Composite PCL/HA/simvastatin electrospun nanofiber coating on biodegradable Mg alloy for orthopedic implant application. J. Coat. Technol. Res. 16 (2), 477–489. https://doi.org/10.1007/s11998-018-0126-8.

Ruan, H., Li, B., Ji, J., Sotto, A., Van der Bruggen, B., Shen, J., Gao, C., 2018. Preparation and characterization of an amphiphilic polyamide nanofiltration membrane with improved antifouling properties by two-step surface modification method. RSC Adv. 8 (24), 13353–13363. https://doi.org/10.1039/C8RA00637G.

Safarpour, M., Khataee, A., Vatanpour, V., 2014. Preparation of a novel polyvinylidene fluoride (PVDF) ultrafiltration membrane modified with reduced graphene Oxide/Titanium dioxide (TiO2) nanocomposite with enhanced hydrophilicity and antifouling properties. Ind. Eng. Chem. Res. 53 (34), 13370–13382. https://doi.org/10.1021/ie502407g.

Said, N., Hasbullah, H., Ismail, A.F., Othman, M.H.D., Goh, P.S., Zainol Abidin, M.N., et al., 2017. Enhanced hydrophilic polysulfone hollow fiber membranes with addition of iron oxide nanoparticles. Polym. Int. 66 (11), 1424–1429. https://doi.org/10.1002/pi.5401.

Scott, K., 1995. Introduction to membrane separations. In: Scott, K. (Ed.), Handbook of Industrial Membranes. Elsevier Science, Amsterdam, pp. 3–185.

Song, H.J., Jo, Y.J., Kim, S.-Y., Lee, J., Kim, C.K., 2014. Characteristics of ultrafiltration membranes fabricated from polysulfone and polymer-grafted silica nanoparticles: effects of the particle size and grafted polymer on the membrane performance. J. Memb. Sci. 466, 173–182. https://doi.org/10.1016/j.memsci.2014.04.053.

Su, C., Xu, Y., Zhang, W., Liu, Y., Li, J., 2012. Porous ceramic membrane with super-hydrophobic and superoleophilic surface for reclaiming oil from oily water. Appl. Surf. Sci. 258 (7), 2319–2323. https://doi.org/10.1016/j.apsusc.2011.10.005.

Ulbricht, M., 2006. Advanced functional polymer membranes. Polymer 47 (7), 2217–2262. https://doi.org/10.1016/j.polymer.2006.01.084.

Wang, J., Dlamini, D.S., Mishra, A.K., Pendergast, M.T.M., Wong, M.C.Y., Mamba, B.B., et al., 2014. A critical review of transport through osmotic membranes. J. Memb. Sci. 454, 516–537. https://doi.org/10.1016/j.memsci.2013.12.034.

Yang, H.-C., Waldman, R.Z., Chen, Z., Darling, S.B., 2018. Atomic layer deposition for membrane interface engineering. Nanoscale 10 (44), 20505–20513. https://doi.org/

10.1039/C8NR08114J.

Zhao, S., Wang, Z., Wei, X., Zhao, B., Wang, J., Yang, S., Wang, S., 2011. Performance improvement of polysulfone ultrafiltration membrane using PANiEB as both pore forming agent and hydrophilic modifier. J. Memb. Sci. 385-386, 251–262. https://doi.org/10.1016/j.memsci.2011.10.006.

Zhao, J., Su, Y., He, X., Zhao, X., Li, Y., Zhang, R., Jiang, Z., 2014. Dopamine composite nanofiltration membranes prepared by self-polymerization and interfacial poly-merization. J. Memb. Sci. 465, 41–48. https://doi.org/10.1016/j.memsci.2014.04.018.